Inorganic Chemistry

pubs.acs.org/IC

Communication

The Smallest Polyoxotungstate Retained by TRIS-Stabilization

Nadiia I. Gumerova, Alexander Prado-Roller, Mark A. Rambaran, C. André Ohlin, and Annette Rompel*

Cite This: *Inorg. Chem.* 2021, 60, 12671−12675

Read Online

ACCESS | Metrics & More | Article Recommendations | Supporting Information

ABSTRACT: A polycondensation reaction of the orthotungstate anion WO_4^{2-}, buffered at pH 7.5 in a TRIS-HCl (0.15 M) solution, results in the first example of a discrete polyoxotungstate anion, with just two W ions stabilized with TRIS ligands. It was isolated and characterized as $Na_2[W^{VI}_2O_6(C_4O_3NH_{10})_2]\cdot 6H_2O$ by single-crystal and powder X-ray diffraction, FT-IR spectroscopy, thermogravimetrical analysis (TGA), and elemental analysis in solid state and by electro-spray ionization mass spectrometry (ESI-MS), ^{13}C, and ^{183}W NMR, as well as Raman spectroscopy in solution. This synthesis demonstrates the crucial and new role of the added tris-alkoxy ligand in the development of a new hybrid TRIS-isopolytungstate with the lowest known nuclearity (so far) and the terminal oxygens substituted with two nitrogen atoms arising from amines of the TRIS ligands.

Polyoxometalates (POMs) are discrete anionic molecular metal-oxide clusters that are usually composed of group V and VI transition metals in their highest oxidation states and exist at the unique interface between monomeric oxometalates and polymeric metal oxides[1] exhibiting a wide range of applications.[2] There are three main criteria by which a metal oxide can be called a POM: (1) addenda ions have quasi-octahedral-coordination and form d_π-p_π bonds with oxygen atoms,[1] (2) two octahedra are connected via sharing the edge, and (3) each octahedral unit has just two terminal O atoms.[3] Oxygen atoms are the primary ligands for the addenda metals in POMs; however, replacing them with other elements while maintaining the structure is possible. So far, many synthesis procedures of oxo-replaced POM structures require water-free organic solvents and the overwhelming majority of POMs with nitrogen atoms bound to the addenda ion are polyoxomolybdates (POMos)[4] or polyoxovanadates (POVs).[5] Attempts to directly functionalize $[W_6O_{19}]^{2-}$ polyoxotungstate (POT) have failed when applying imido approaches suitable for POMos and POVs, since $[W_6O_{19}]^{2-}$ does not react with phosphinimines, isocyanates, or primary amines.[4]

In solution, small and stable POMs are interesting as useful building blocks for constructing huge metal−oxo clusters.[6] In many cases, polycondensation reactions of $[MO_x]^{n-}$ (M = addenda ion) immediately lead to larger structures, and POMs with low nuclearity are quite elusive.[1] In acidified solutions of WO_4^{2-}, both in the presence or absence of heteroions, anions with less than six W are underrepresented.[7−10] The smallest discrete isopolytungstates (IPOT) verified to exist both in the solid state and in solutions are the Lindqvist hexatungstate $[W_6O_{19}]^{2-}$ in nonaqueous media and heptatungstate $[W_7O_{24}]^{6-}$ in water.[1,7] Discrete binuclear complexes of pentavalent tungsten $[W^V_2O_4(Y)]^{2-}$ (Y^{4-} = hexadentate ligand, e.g., ethylenediaminetetraacetate) in octahedral coordination are known;[11] however, they have not been obtained by acidification of orthotungstate. The strategy of using organic ligands to inhibit the formation of large clusters has previously been applied to POMos[12] and POVs[13] while it has not been reported for POTs. Tris(hydroxymethyl)aminomethane ($(HOCH_2)_3CNH_2$, TRIS) has been recently utilized to stabilize and isolate elusive heptavanadate.[13] While in biochemistry, TRIS (pK_a 8.06) is used as pH buffer between 7.0 and 9.2,[14] in POM chemistry, TRIS is usually used for covalent organic functionalization via alkoxo-groups $-CH_2OH$ attachment to the POM,[15−17] and $-NH_2$ plays the key role for postfunctionalization through amide bond formation.[18−20] Recently, we expanded the role of TRIS by showing that TRIS, as part of a buffer solution that is normally considered unimportant, plays a defining role in the formation of a new member of the Keggin family.[21] In POM chemistry, TRIS has never acted as a primary amine by replacing oxo-ligands and thus as a protective ligand to prevent the formation of POTs with a higher nuclearity.

A discrete small anion, which is additionally organically functionalized for better stability, could be an ideal candidate for its use as a building block. To synthesize such an anion, we investigated an IPOT formation in a TRIS buffered solution (pH 7.5, 0.15 M) of WO_4^{2-}. Herein, we report for the first time the successful synthesis of the discrete $[W^{VI}_2O_6(C_4O_3NH_{10})_2]^{2-}$ (**W_2**), which meets all the requirements to be called a POM[1] (W^{VI} has quasi-octahedral-coordination; two octahedra are connected via sharing the edge; W^{VI} has just two terminal O atoms) and is the smallest POT hybridized with TRIS known so far. **W_2** is a representative of a POM family with replaced oxygen ions by other nonmetals and the first POT functionalized directly by a primary amine in aqueous solution.

Initially, 12 mL of an aqueous solution of WO_4^{2-} (0.188 M) was acidified with HCl (1 M) to pH 4.4 followed by the

Received: April 18, 2021
Published: June 14, 2021

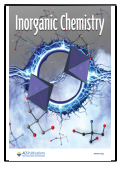

https://doi.org/10.1021/acs.inorgchem.1c01188
Inorg. Chem. 2021, 60, 12671−12675

addition of TRIS (0.3 g, 2.5 mmol, 0.15 M) that led to an increase in pH to 7.5 (Figure 1A). After the final mixture was

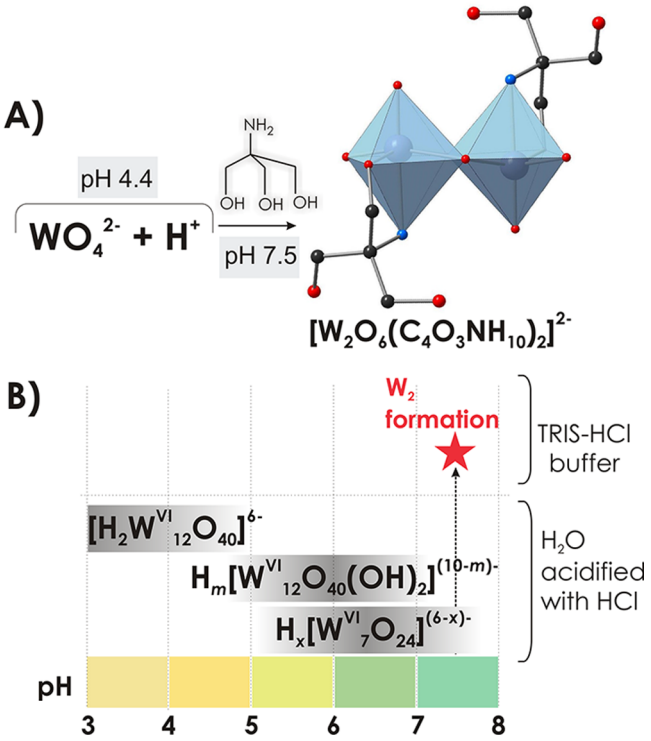

Figure 1. Synthetic route to prepare $\mathbf{W_2}$ (**A**) and the speciation diagram in buffered and unbuffered[7] aqueous solution of WO_4^{2-} in the pH range from 3 to 8 (**B**). Color code: {WO_6}, light blue; O, red; N, blue; C, black.

heated for 1 h at 90 °C and kept at room temperature, colorless crystals of $Na_2[W^{VI}_2O_6(C_4O_3NH_{10})_2]\cdot 6H_2O$ ($\mathbf{Na_2W_2}$) were formed. Single crystal structure analysis of $\mathbf{W_2}$ revealed that TRIS acts not only as a buffer component but also as a shielding ligand, preventing formation of IPOTs with a higher nuclearity in unbuffered WO_4^{2-} solution, namely, $H_x[W^{VI}_{12}O_{40}(OH)_2]^{(10-x)-}$ (x = 0–3) and $[H_2W^{VI}_{12}O_{40}]^{6-}$ between pH 2 and 5 as well as $[W^{VI}_7O_{24}]^{6-}$ and $[W^{VI}_{12}O_{40}(OH)_2]^{10-}$ at pH 7.5 (Figure 1B).[7−9]

$\mathbf{Na_2W_2}$ crystallizes in the triclinic space group $P\bar{1}$ (CCDC 2078090). The structure is composed of a $[W^{VI}_2O_6(C_4O_3NH_{10})_2]^{2-}$ and two Na^+, connected to the tungsten cluster via O–CH_2 groups of TRIS and forming a {NaO_5} polyhedron (Figure 2). The coordination environment of each W^{VI} consists of two terminal O_t (d(W1–O4) = 1.766 Å, d(W1–O5) = 1.767 Å), two bridging μ_2-O (d(W1–O6) = 1.858 and 2.167 Å), one oxygen atom, and one nitrogen atom (d(W1–N1) = 2.344 Å) from one TRIS molecule (Figure 2). The W–N bond lengths in $\mathbf{Na_2W_2}$ are slightly longer than those previously reported in POTs (2.13 to 2.17 Å),[22,23] indicating the weaker π contribution of the bonds.[24] The W–W bond length is 3.194 Å, which is shorter than that in classical IPOTs.[9,21]

The stretching vibrations of the W=O units are present at 919 cm^{-1} in the IR spectrum of $Na_2\mathbf{W_2}$ (Figure S1). The bands at 894 cm^{-1} and in the region from 470 to 750 cm^{-1} correspond to the antisymmetric and symmetric deformation vibrations of W–O–W. The three bands at 1084, 1059, and 1040 cm^{-1} are assigned to C–O stretching vibrations,

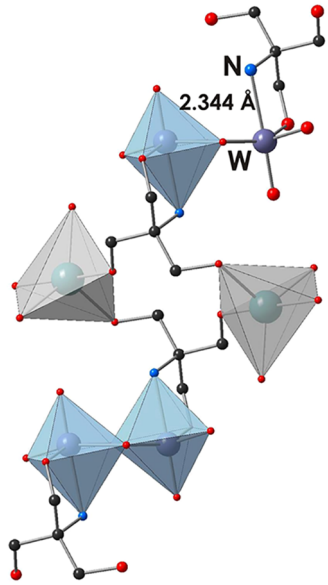

Figure 2. Binding of $\mathbf{W_2}$ to Na^+ through the $-CH_2OH$ groups of TRIS ligands. Color code: W, purple; {WO_6}, blue; {NaO_5}, gray; O, red; N, blue; C, black.

indicating the successful grafting of TRIS. TGA was used to examine the weight loss and thermal stability of the synthesized hybrid POT. The TG curve shows four weight-loss regions up to 700 °C due to dehydration followed by disintegration of TRIS (Figure S2). The experimental and simulated X-ray diffraction patterns of $Na_2\mathbf{W_2}$ (Figure S3) fit perfectly in the range from 10 to 50° 2θ confirming its homogeneity.

The stability of $\mathbf{W_2}$ in H_2O at pH 6.8 was investigated by ESI-MS (Figures 3, S4, S5, and Table S2). The ESI-MS spectrum recorded in positive mode exhibits three series of peaks' envelopes at m/z between 400 and 850, which can be unambiguously assigned to the singly charged cations (Figure 3, Table S2). The first group of signals (m/z = 439.1, 461.1, 479.1, 501.0) corresponds to the monomeric complex $[W^{VI}(C_4O_3NH_8)_2]^0$ in which two TRIS are coordinated to W^{VI} via $-CH_2O$- groups (blue in Figure 3). The signals at 711.0, 733.0, and 755.0 m/z correspond to the $\mathbf{W_2}$ (purple in Figure 3) in which one more $-CH_2OH$ fragment is attached to one of the equivalent W^{VI}. The $\mathbf{W_2}$ with the symmetrical attachment of two additional $-CH_2OH$ (green in Figure 3) gives signals at 792.1, 814.1, 832.1, and 854.1 m/z. The attachment of TRIS ligands through three functional groups to the trimeric face of W^{VI} ions is a known strategy in POM chemistry for elusive anion stabilization[13] and may be the reason that these compounds are detected in solution. The ESI-MS spectrum of $Na_2\mathbf{W_2}$ recorded in the negative mode (Figure S4) demonstrates the absence of signals from any IPOTs.

To further examine the solution behavior of $\mathbf{W_2}$, ^{13}C and ^{183}W NMR spectroscopic studies were performed in D_2O at pH 7.5 (Figures S6 and S7). The ^{183}W NMR spectrum of $Na_2\mathbf{W_2}$ (0.058 M) in D_2O shows one intense signal with a chemical shift at −3.4 ppm and one minor signal at −91.9 ppm (Figure S6A). Since there exist no reference spectra for POTs with two equivalent W atoms and the chemical shift in $\mathbf{Na_2W_2}$ spectrum is very close to 0 ppm (reference Na_2WO_4), a ^{183}W NMR spectrum for the equimolar mixture of $\mathbf{W_2}$ and WO_4^{2-}

https://doi.org/10.1021/acs.inorgchem.1c01188
Inorg. Chem. 2021, 60, 12671−12675

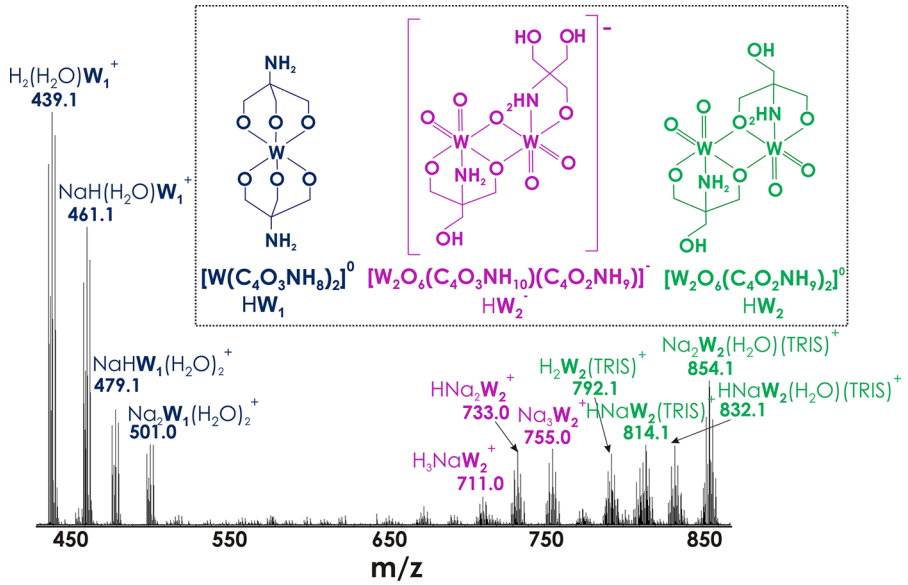

Figure 3. ESI mass spectrum of $Na_2\mathbf{W_2}$ in H_2O (pH 6.8) recorded in the positive mode in the range from 430 to 860 m/z. Three types of species are shown in blue, purple, and green. Figure S5 shows the spectrum in the range from 100 to 1000 m/z, and Table S2 provides all species with experimental and theoretical m/z values.

was acquired. The spectrum of the mixture demonstrates the same two signals at −2.8 and −91.6 ppm and one additional signal at −53.4 ppm (Figure S6B). The signal at −91.6 ppm can be attributed to $[W^{VI}{}_7O_{24}]^{6-}$, which gives three signals at 268.8, −90.9, and −180.2 (Figure S6D). The spectrum of $\mathbf{W_2}$ recorded in NaOAc/50% D_2O at pH 6 (Figure S6C), where no signal for WO_4^{2-} should be observed (Figure 1B), shows a very intense signal at −2.1 ppm. DFT calculations have been performed to assign the peaks to tungsten species (Table S3). A comparison of calculated and experimental values for $[W^{VI}{}_6O_{19}]^{2-}$, WX_6 (X = F^-, Cl^-, CO) and for $\mathbf{W_2}$ shows that the calculated shift of −17 ppm can be attributed to the signal around 0 ppm if assigned to $\mathbf{W_2}$. The ^{13}C NMR spectrum of $Na_2\mathbf{W_2}$ in D_2O (pH 7.5) shows two signals at 59.8 and 60.8 ppm (Figure S7B), which do not correspond to the $\mathbf{W_2}$ structure observed in the solid state, where three types of carbons are present (Figure 2). However, the signals at 59.8 and 60.8 ppm also cannot be attributed to the free TRIS with signals at 56.4 and 63.0 ppm (Figure S7A). In the $Na_2\mathbf{W_2}$ solution at pH 6, the ^{13}C NMR spectrum shows three signals at 59.3, 61.4, and 63.4 ppm, which indicate potential ligand binding according to the $\mathbf{W_2}$ structure (Figure 2). Raman spectroscopy was performed in the solid state and in solution to support ESI-MS and NMR spectroscopic data. The Raman spectrum of $Na_2\mathbf{W_2}$ in H_2O (pH 7.5) points to its dissociation to orthotungstate WO_4^{2-} (Figure 4). On the basis of DFT calculations, ESI-MS, and NMR and Raman spectroscopy, we argue that $\mathbf{W_2}$ is unstable in an aqueous solution at pH 7.5; however, some intermediates detected by ESI-MS (Figure 3) with another type of TRIS attachment are at least partially present in slightly acidic solutions.

Considering the facile and reproducible synthesis of $\mathbf{W_2}$, as well as its small size, there are two scenarios for the use of $\mathbf{W_2}$ in the future for the formation of novel metal-oxide-based materials. One possible route is based on the rigid $\mathbf{W_2}$ nature, which is similar to that of the dinuclear $[M^V{}_2S_2O_2(H_2O)_6]^{2+}$ (M = Mo or W),[25,26] rendering $\mathbf{W_2}$ a potential connecting building block. The second scenario aims to expand the existing oxo-replaced POM chemistry. The strategy using the

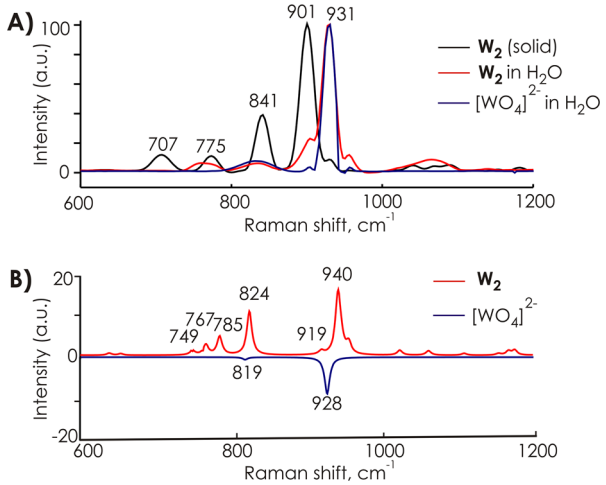

Figure 4. Experimental (**A**) and computed (**B**) Raman spectra of $Na_2[W^{VI}{}_2O_6(C_4O_3NH_{10})_2]\cdot 6H_2O$ ($\mathbf{Na_2W_2}$) and Na_2WO_4 in the range from 600 to 1200 cm^{-1}. Solution spectra were recorded in H_2O with pH 7.5 in $\mathbf{Na_2W_2}$.

reaction of lacunary Keggin anion $[PW_{11}O_{39}]^{7-}$ with the mononuclear imido-tungsten precursor $[W^{VI}(NC_6H_5)Cl_4]$ was successfully applied[27] and can be taken as a model for $\mathbf{W_2}$.

In conclusion, the existence of the anion just with two tungsten ions, which fulfills all criteria to be called POM, has been demonstrated for the first time, where W(VI) ion is coordinated to two TRIS molecules through W−N and W−O chemical bonds. Full characterizations in the solid state and in solution elucidate the composition and solution behavior of the $\mathbf{W_2}$ anion.

■ ASSOCIATED CONTENT

Supporting Information

The Supporting Information is available free of charge at https://pubs.acs.org/doi/10.1021/acs.inorgchem.1c01188.

https://doi.org/10.1021/acs.inorgchem.1c01188
Inorg. Chem. 2021, 60, 12671−12675

Synthetic details and spectroscopic data along with structural characterizations of the new compound (PDF)

Accession Codes

CCDC 2078090 contains the supplementary crystallographic data for this paper. These data can be obtained free of charge via www.ccdc.cam.ac.uk/data_request/cif, or by emailing data_request@ccdc.cam.ac.uk, or by contacting The Cambridge Crystallographic Data Centre, 12 Union Road, Cambridge CB2 1EZ, UK; fax: + 44 1223 336033.

AUTHOR INFORMATION

Corresponding Author

Annette Rompel − *Universität Wien, Fakultät für Chemie, Institut für Biophysikalische Chemie, 1090 Wien, Austria;* orcid.org/0000-0002-5919-0553; Email: annette.rompel@univie.ac.at; http://www.bpc.univie.ac.at

Authors

Nadiia I. Gumerova − *Universität Wien, Fakultät für Chemie, Institut für Biophysikalische Chemie, 1090 Wien, Austria*

Alexander Prado-Roller − *Universität Wien, Fakultät für Chemie, Zentrum für Röntgenstrukturanalyse und Institut für Anorganische Chemie, 1090 Wien, Austria*

Mark A. Rambaran − *Umeå University, Department of Chemistry, 901 87 Umeå, Sweden*

C. André Ohlin − *Umeå University, Department of Chemistry, 901 87 Umeå, Sweden*

Complete contact information is available at: https://pubs.acs.org/10.1021/acs.inorgchem.1c01188

Author Contributions

The manuscript was written through contributions of all authors. All authors have given approval to the final version of the manuscript.

Funding

This research was funded by the Austrian Science Fund (FWF): P33927 (N.G.) and P33089 (A.R.) and the University of Vienna.

Notes

The authors declare no competing financial interest.

ACKNOWLEDGMENTS

We thank Ao.Univ.-Prof. Dr. Markus Galanski for great support with ^{183}W NMR spectroscopic data collection at the NMR Core Facility, Elias Tanuhadi, MSc for PXRD measurements, Ass.-Prof. Dr. Peter Unfried for TGA and Mag. A. Fabisikova for ESI-MS measurements at the MS Center, Faculty of Chemistry, University of University of Vienna, and Florian Gregor Covi, BSc for speciation studies during his practical course.

DEDICATION

Dedicated to Dr. sc. nat. Hans-Joachim Lunk on the occasion of his 80th birthday.

REFERENCES

(1) Pope, M. T. Inorganic Chemistry Concepts. *Heteropoly and Isopoly Oxometalates*; Springer: Berlin, 1983; Vol. *8*.

(2) (a) Bijelic, A.; Aureliano, M.; Rompel, A. Polyoxometalates as potential next-generation metallodrugs in the combat against cancer. *Angew. Chem., Int. Ed.* **2019**, *58*, 2980−2999; *Angew. Chem.* **2019**, *131*, 3008−3029. (b) Bijelic, A.; Aureliano, M.; Rompel, A. The antibacterial activity of polyoxometalates: structures, antibiotic effects and future perspectives. *Chem. Commun.* **2018**, *54*, 1153−1169. (c) Wang, S. S.; Yang, G. Y. Recent advances in polyoxometalate-catalyzed reactions. *Chem. Rev.* **2015**, *115*, 4893−4962. (d) Horn, M. R.; Singh, A.; Alomari, S.; Goberna-Ferrón, S.; Benages-Vilau, R.; Chodankar, N.; Motta, N.; Ostrikov, K.; MacLeod, J.; Sonar, P.; Gomez-Romero, P.; Dubal, D. Polyoxometalates (POMs): from electroactive clusters to energy materials. *Energy Environ. Sci.* **2021**, *14*, 1652−1700.

(3) Lipscomb, W. N. Paratungstate ion. *Inorg. Chem.* **1965**, *4*, 132−134.

(4) Zhang, J.; Xiao, F.; Hao, J.; Wei, Y. The chemistry of organoimido derivatives of polyoxometalates. *Dalton Trans.* **2012**, *41*, 3599−3615.

(5) Khan, M. I.; Tabussum, S.; Doedens, R. J.; Golub, V. O.; O'Connor, C. J. Functionalized metal oxide clusters: Synthesis, characterization, crystal structures, and magnetic properties of a novel series of fully reduced heteropolyoxovanadium cationic clusters decorated with organic ligands- $[MV^{IV}_6O_6\{(OCH_2CH_2)_2N(CH_2CH_2OH)\}_6]X$ (M = Li, X = Cl·LiCl; M = Na, X = Cl·H_2O; M = Mg, X = 2Br·H_2O; M = Mn, Fe, X = 2Cl; M = Co, Ni, X = 2Cl·H_2O). *Inorg. Chem.* **2004**, *4*, 5850−5859.

(6) Miras, H. N.; Yan, J.; Long, D.-L.; Cronin, L. Structural evolution of "S"-shaped $[H_4W_{22}O_{74}]^{12-}$ and "§"-Shaped $[H_{10}W_{34}O_{116}]^{18-}$ isopolyoxotungstate clusters. *Angew. Chem., Int. Ed.* **2008**, *47*, 8420−8423.

(7) Gumerova, N. I.; Rompel, A. Polyoxometalates in solution: speciation under spotlight. *Chem. Soc. Rev.* **2020**, *49*, 7568−7601.

(8) Hastings, J. J.; Howarth, O. W. A ^{183}W, ^{1}H and ^{17}O nuclear magnetic resonance study of aqueous isopolytungstates. *J. Chem. Soc., Dalton Trans.* **1992**, 209−215.

(9) Rozantsev, G. M.; Radio, S. V.; Gumerova, N. I. Strontium isopoly tungstates: Synthesis and properties. *Pol. J. Chem.* **2008**, *82*, 2067−2080

(10) Liu, Y.-J.; Jin, M.-T.; Chen, L.-J.; Zhao, J.-W. Recent advances in isopolyoxotungstates and their derivatives. *Acta Crystallogr., Sect. C: Struct. Chem.* **2018**, *C74*, 1202−1221.

(11) (a) Novák, J.; Podlaha, J. Tungsten(V) complexes of ethylenediaminetetraacetic acid. *J. Inorg. Nucl. Chem.* **1974**, *36*, 1061−1065. (b) Saito, K.; Sasaki, Y.; Hazama, R. Doubly-bridged binuclear complexes of oxomolybdenum(V) and oxotungsten(V) containing sexadentate ligands. *J. Cluster Sci.* **1995**, *6*, 549−566.

(12) Long, D.-L.; Kögerler, P.; Farrugia, L. J.; Cronin, L. Restraining symmetry in the formation of small polyoxomolybdates: New building blocks of unprecedented topology resulting from shrink-wrapping $[H_2Mo_{16}O_{52}]^{10-}$ type clusters. *Angew. Chem., Int. Ed.* **2003**, *42*, 4180−4183.

(13) Fernández-Navarro, L.; Nunes-Collado, A.; Artetxe, B.; Ruiz-Bilbao, E.; San Felices, L.; Reinoso, S.; San José Wéry, A.; Gutiérrez-Zorrilla, J. M. Isolation of the Elusive Heptavanadate Anion with Trisalkoxide Ligands. *Inorg. Chem.* **2021**, *60*, 5442−5445.

(14) Bubb, W. A.; Berthon, H. A.; Kuchel, P. W. Tris Buffer Reactivity with Low-Molecular-Weight Aldehydes: NMR Characterization of the Reactions of Glyceraldehyde-3-Phosphate. *Bioorg. Chem.* **1995**, *23*, 119−130.

(15) Zhang, J.; Huang, Y.; Li, G.; Wei, Y. Recent advances in alkoxylation chemistry of polyoxometalates: From synthetic strategies, structural overviews to functional applications. *Coord. Chem. Rev.* **2019**, *378*, 395−414.

(16) (a) Blazevic, A.; Al-Sayed, E.; Roller, A.; Giester, G.; Rompel, A. Tris−functionalized hybrid Anderson polyoxometalates: synthesis, characterization, hydrolytic stability and inversion of protein surface charge. *Chem. - Eur. J.* **2015**, *21*, 4762−4771. (b) Gumerova, N. I.; Roller, A.; Rompel, A. Synthesis and characterization of the first Ni(II)-centered single-side tris-functionalized Anderson-type polyoxomolybdate. *Eur. J. Inorg. Chem.* **2016**, *36*, 5507−5511.

(17) (a) Gumerova, N. I.; Roller, A.; Rompel, A. [Ni(OH)$_3$W$_6$O$_{18}$(OCH$_2$)$_3$CCH$_2$OH]$^{4-}$: the first tris-functionalized Anderson-type heteropolytungstate. *Chem. Commun.* **2016**, *52*, 9263−9266. (b) Gumerova, N. I.; Caldera Fraile, T.; Roller, A.; Giester, G.; Pascual-Borràs, M.; Ohlin, C. A.; Rompel, A. The direct single- and double-side triol-functionalization of the mixed type Anderson polyoxotungstate [Cr(OH)$_3$W$_6$O$_{21}$]$^{6-}$. *Inorg. Chem.* **2019**, *58*, 106−113.
(18) Anyushin, A. V.; Kondinski, A.; Parac-Vogt, T. N. Hybrid polyoxometalates as post-functionalization platforms: from fundamentals to emerging applications. *Chem. Soc. Rev.* **2020**, *49*, 382−432.
(19) (a) Al-Sayed, E.; Blazevic, A.; Roller, A.; Rompel, A. The synthesis and characterization of aromatic hybrid Anderson-Evans POMs and their serum albumin interaction - The shift from polar to hydrophobic interactions. *Chem. - Eur. J.* **2015**, *21*, 17800−17807. (b) Gumerova, N. I.; Blazevic, A.; Caldera Fraile, T.; Roller, A.; Giester, G.; Rompel, A. Synthesis and Characterization of Hybrid Anderson Hexamolybdoaluminates (III) Functionalized with Indometacin or Cinnamic Acid. *Acta Crystallogr., Sect. C: Struct. Chem.* **2018**, *74*, 1378−1383.
(20) Bijelic, A.; Dobrov, A.; Roller, A.; Rompel, A. Binding of a fatty acid functionalized Anderson-type polyoxometalate to human serum albumin. *Inorg. Chem.* **2020**, *58*, 5243−5246.
(21) Gumerova, N. I.; Roller, A.; Giester, G.; Krzystek, J.; Cano, J.; Rompel, A. Incorporation of Cr^{III} into a Keggin polyoxometalate as a chemical strategy to stabilize a labile {Cr^{III}O$_4$} tetrahedral conformation and promote unattended single-ion magnet properties. *J. Am. Chem. Soc.* **2020**, *142*, 3336−3339.
(22) Suzuki, K.; Shinoe, M.; Mizuno, N. Synthesis and Reversible Transformation of Cu$_n$-Bridged (n = 1, 2, or 4) Silicodecatungstate Dimers. *Inorg. Chem.* **2012**, *51*, 11574−11581.
(23) Suzuki, K.; Minato, T.; Tominaga, N.; Okumo, I.; Yonesato, K.; Mizuno, N.; Yamaguchi, K. Hexavacant γ-Dawson-type phosphotungstates supporting an edge-sharing bis(square-pyramidal) {O$_2$M(μ_3-O)$_2$(μ-OAc)MO$_2$} core (M = Mn^{2+}, Co^{2+}, Ni^{2+}, Cu^{2+}, or Zn^{2+}). *Dalton Trans.* **2019**, *48*, 7281−7289.
(24) Li, C.; Mizuno, N.; Yamaguchi, K.; Suzuki, K. Self-Assembly of Anionic Polyoxometalate−Organic Architectures Based on Lacunary Phosphomolybdates and Pyridyl Ligands. *J. Am. Chem. Soc.* **2019**, *141*, 7687−7692.
(25) Cadot, E.; Sokolov, M. N.; Fedin, V. P.; Simonnet-Jégat, C.; Floquet, S.; Sécheresse, F. A building block strategy to access sulfur-functionalized polyoxometalate based systems using {Mo$_2$S$_2$O$_2$} and {Mo$_3$S$_4$} as constitutional units, linkers or templates. *Chem. Soc. Rev.* **2012**, *41*, 7335−7353.
(26) Béreau, V.; Cadot, E.; Bögge, H.; Müller, A.; Sécheresse, F. Addition of {M$_2$S$_2$O$_2$}$^{2+}$, M = Mo, W, to A-α-[PW$_9$O$_{34}$]$^{9-}$. Synthesis and structural characterizations in the solid state and in solution. *Inorg. Chem.* **1999**, *38*, 5803−5808.
(27) Duhacek, J. C.; Duncan, D. C. Phenylimido Functionalization of α-[PW$_{12}$O$_{40}$]$^{3-}$. *Inorg. Chem.* **2007**, *46*, 7253−7255.

https://doi.org/10.1021/acs.inorgchem.1c01188
Inorg. Chem. 2021, 60, 12671−12675